

iScience, Volume 26

## **Supplemental information**

### **Mitochondrial network adaptations of microglia reveal sex-specific stress response after injury and UCP2 knockout**

**Margaret E. Maes, Gloria Colombo, Florianne E. Schoot Uiterkamp, Felix Sternberg, Alessandro Venturino, Elena E. Pohl, and Sandra Siegert**

# Figure S1.

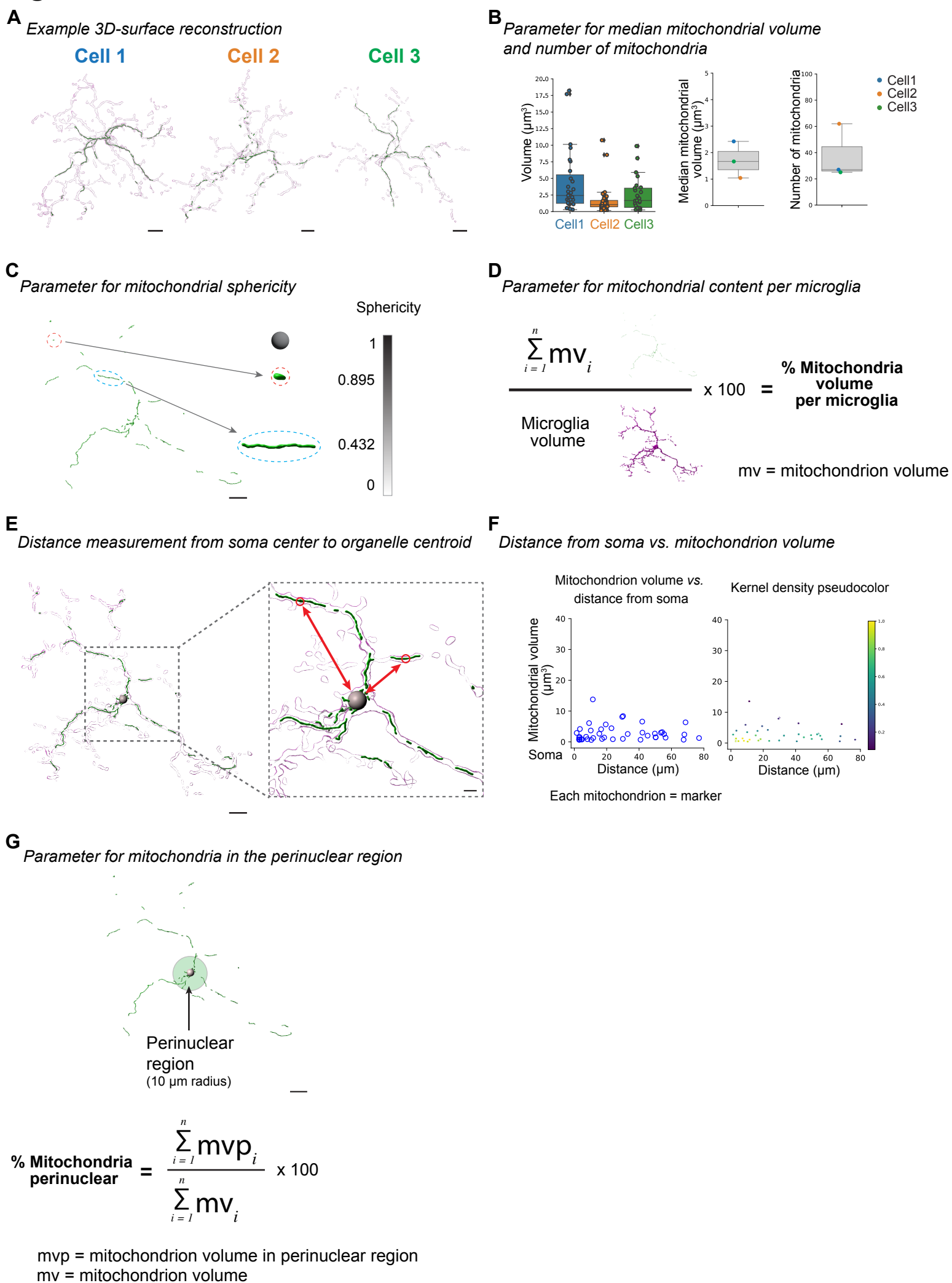


## Figure S1. Analyzed mitochondrial parameters in microglia, Related to Figure 1

Introduction to the mitochondrial parameters based on three 3D-surface reconstructions of IBA1-immunostained microglia (magenta) from IPL WT (magenta) expressing mito-Dendra2 (green, **A**). Scale bar: 10  $\mu\text{m}$ .

**(B)** Left, boxplot for each cell indicating the volume of every mitochondrial organelle per cell. Each dot, a mitochondrion. Center, median mitochondrial volume and right, number of mitochondria for each cell at left. Boxplot minimum and maximum: InterQuartile Range (IQR) around median (center line). Whiskers: 1.5 IQRs. Black diamond points: outliers outside 1.5 IQRs.

**(C)** Mitochondrial sphericity. Left, example mitochondrial 3D-surface (green) from a WT microglia. Ratio of mitochondrion volume to mitochondrion surface area represents sphericity with two exemplar organelles (orange, sphericity = 0.895) and elongated (blue, sphericity = 0.432). Sphericity is represented as a mean sphericity value of all mitochondria per cell. Scale bar: 15  $\mu\text{m}$ .

**(D)** Percentage of the sum of mitochondrial volume in a cell (**Figure S1B, left**) over the microglial volume represents mitochondrial content per cell.

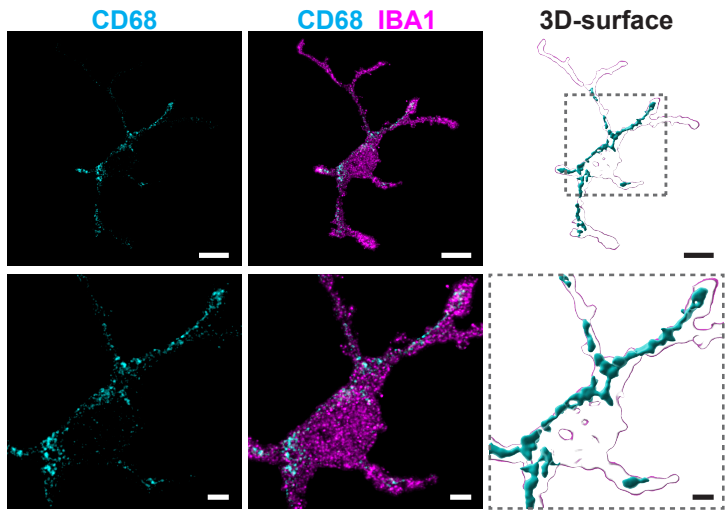
**(E)** Vesicle distance measurement. Example 3D-volume surfaces of an IBA1-immunostained microglia (magenta) with mito-Dendra2 expression (green). Grey sphere: cell soma. Right, zoom-in of region of interest (dashed line). Example red circles: centroid of mitochondrion. Arrows: distance from centroid to soma determined from the centroid of each mitochondrion/vesicle to the center of the soma-sphere (red arrows). Scale bar: 15  $\mu\text{m}$ , zoom-in: 5  $\mu\text{m}$ .

**(F)** Mitochondria or CD68 vesicle localization parameter exemplified using mitochondrial localization. Scatterplot depicts the distance from the soma ( $\mu\text{m}$ ) vs. the mitochondrial volume ( $\mu\text{m}^3$ ) for each mitochondrion shown in (**Figure S1E**). To illustrate overlapping mitochondria, scatterplot markers were pseudo-colored with kernel density estimations.

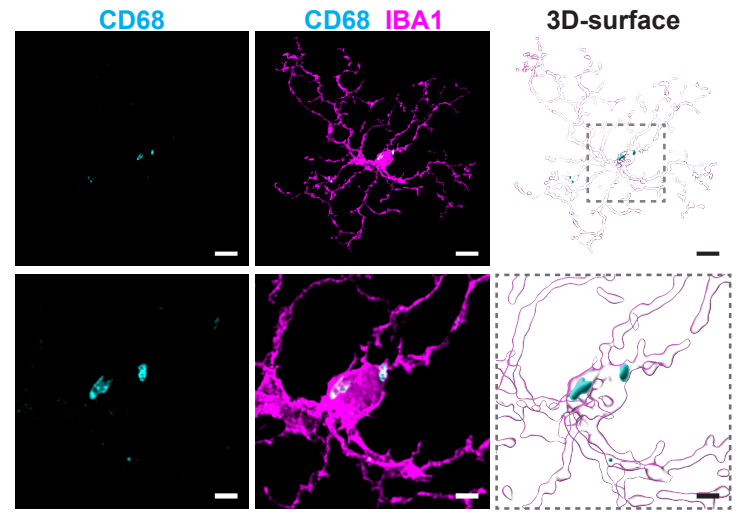
**(G)** Example mitochondrial surface (green) from microglia depicted in (**Figure S1E**). The perinuclear region (shaded green sphere) was determined as the region within a 10  $\mu\text{m}$  radius from the cell soma point. The percentage of mitochondria in the perinuclear region is the sum volume within the perinuclear region over the total mitochondrial volume. Scale bar: 15  $\mu\text{m}$ .

# Figure S2.

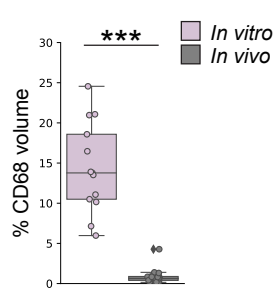
**A** CD68 in microglia *in vitro*



**B** CD68 in microglia *in vivo*



**C** CD68 volume



**D** CD68 localization

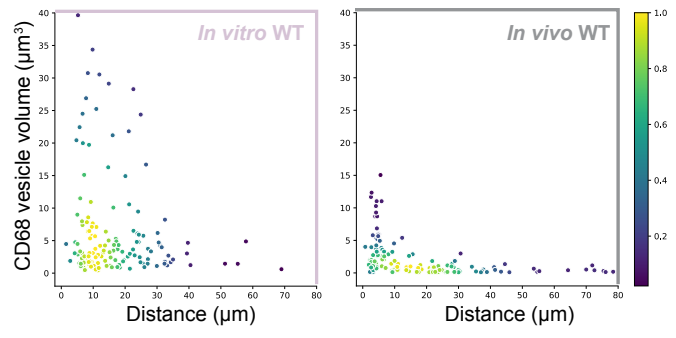


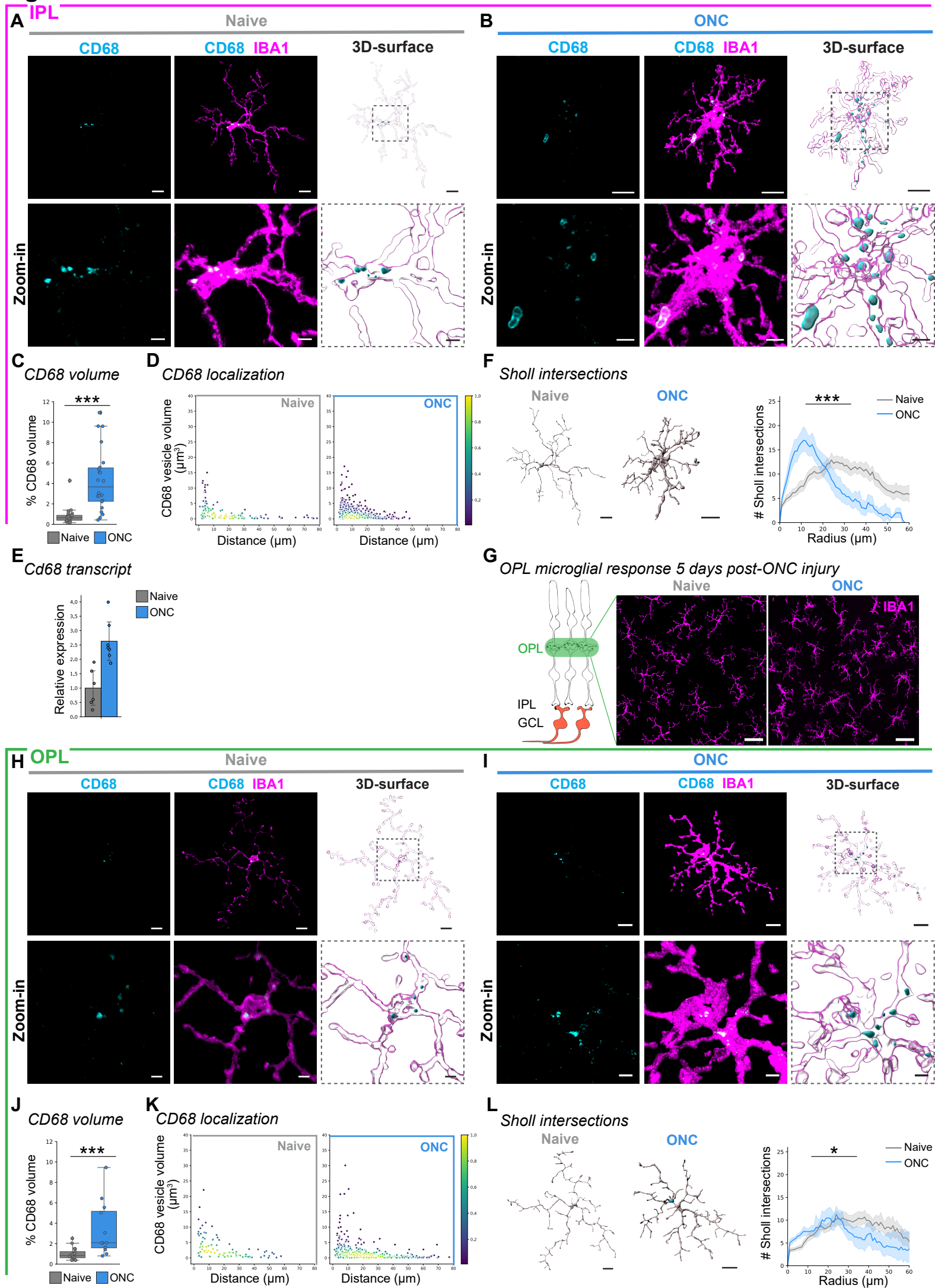
**Figure S2. Microglia *in vitro* exhibit increased CD68 expression, Related to Figure 1**

(A-B) IBA1-immunostained microglia (magenta) from **Figure 1F-G** co-labeled with CD68 (cyan) from *in vitro* (A) or *in vivo* microglia (B). Next, corresponding 3D-surfaces. Below: Zoom-in of region of interest (dashed outline) from image and 3D-surface. Scale bar: 10  $\mu\text{m}$ , zoom-in: 3  $\mu\text{m}$ .

(C) Percentage of total CD68 volume per microglia volume. Boxplot minimum and maximum: InterQuartile Range (IQR) around median (center line). Whiskers: 1.5 IQRs. Black diamond points: outliers outside 1.5 IQRs. Wilcoxon rank sum test:  $p < 0.0001$ .

(D) CD68 vesicle localization. Scatterplot depicting CD68 vesicle volume *vs.* distance from the cell soma (0, origin) of the population of vesicles in *in vitro* (left, dusty pink) and *in vivo* (right, grey) conditions. Point density, pseudo-colored.

\*\*\*  $p < 0.001$ . See **Table S7** for experimental, retina and cell numbers, statistical tests and corresponding data.

**Figure S3.**

## Figure S3. CD68 and microglial morphology changes in ONC-responsive IPL and OPL microglia,

### Related to Figure 2

(A-D, F) Microglial response in IPL WT microglia.

(A-B) Representative IBA1-immunostained IPL microglia (magenta) from **Figure 2D-E** co-labeled with CD68 (cyan) in naïve WT (A, grey) or ONC WT microglia (B, blue). Next, corresponding 3D-surfaces.

Below: Zoom-in of region of interest (dashed line) from image and 3D-surface. Scale bar: 10  $\mu\text{m}$ , zoom-in: 3  $\mu\text{m}$ .

(C) Percentage of total CD68 volume per microglia volume. Boxplot minimum and maximum: InterQuartile Range (IQR) around median (center line). Whiskers: 1.5 IQRs. Black diamond points: outliers outside 1.5 IQRs. Wilcoxon rank sum test:  $p < 0.0001$ .

(D) CD68 vesicle localization. Scatterplot depicting CD68 vesicle volume vs. distance from the cell soma (0, origin) of the population of vesicles in naïve WT (left) and ONC WT (right) conditions. Point density, pseudo-colored.

(E) Bar plot depicting relative *Cd68* transcript expression from FACSed mito-Dendra2<sup>+</sup> microglia in naïve WT or ONC WT retinas. Welch's t-test:  $p = 0.0137$ .

(F) 3D-filament tracings of microglia from naïve WT (left) or ONC WT (right). Scale bar: 10  $\mu\text{m}$ . Line plot for mean number of Sholl intersections per radial distant from the soma ( $\mu\text{m}$ ) with 95% confidence interval band. Linear mixed effects model:  $p < 0.0001$ .

(G) Left, retinal side-view schematic. OPL, outer plexiform layer. IPL, inner plexiform layer. GCL, ganglion cell layer. Overview confocal image of immunostained OPL microglia (IBA1, magenta) in naïve WT (left) and 5 days after ONC WT (right) condition. Scale bar: 30  $\mu\text{m}$ .

(H-L) Microglial response in OPL WT microglia.

(H-I) CD68 (cyan) immunostaining in the IBA1-immunostained OPL microglia (magenta) from **Figure 2I-J** for naïve WT microglia (H) or ONC WT microglia (I). Next, corresponding 3D-surfaces. Below: Zoom-in of region of interest (dashed outline) from image and 3D-surface. Scale bar: 10  $\mu\text{m}$ , zoom-in: 3  $\mu\text{m}$ .

(J) Percentage of total CD68 volume per microglia volume. Boxplot minimum and maximum: InterQuartile Range (IQR) around median (center line). Whiskers: 1.5 IQRs. Black diamond points: outliers outside 1.5 IQRs. Wilcoxon rank sum test:  $p = 0.0007$ .

(K) CD68 vesicle localization. Scatterplot depicting CD68 vesicle volume *vs.* distance from the cell soma (0, origin) of the population of vesicles in naïve (left, grey) and ONC (right, blue) conditions. Point density, pseudo-colored.

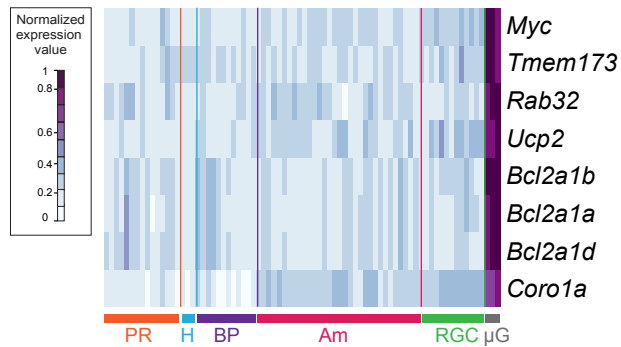
(L) 3D-filament tracings of microglia from naïve WT (left) or ONC WT (right). Scale bar: 10  $\mu\text{m}$ . Line plot for mean number of Sholl intersections per radial distant from the soma ( $\mu\text{m}$ ) with 95% confidence interval band. Linear mixed effects model:  $p = 0.0302$ .

\*  $p < 0.05$ , \*\*\*  $p < 0.001$ . See **Table S8** for retina and cell numbers, statistical tests and corresponding data.

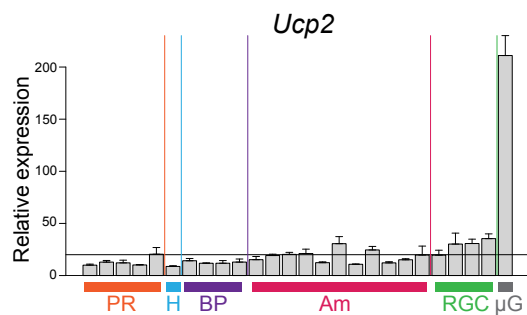


# Figure S4.

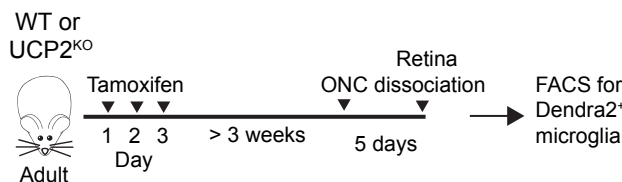
## A Candidate mitochondrial genes enriched in retinal microglia



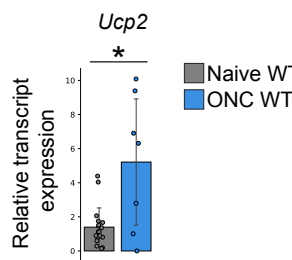
## B Relative Ucp2 expression among retinal cell types



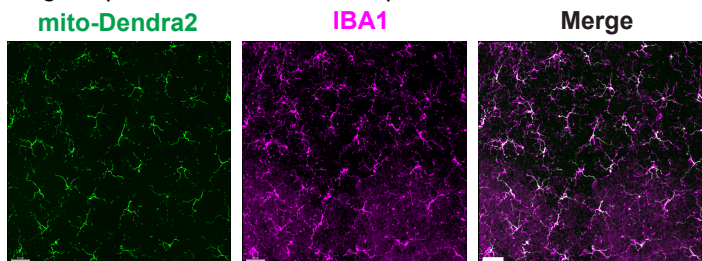
## C Tamoxifen injection timeline for FACS isolation



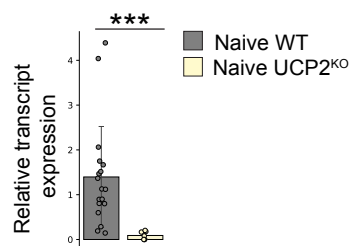
## D Microglial Ucp2 transcript increases upon ONC



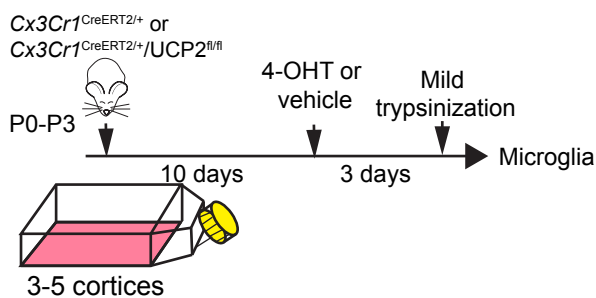
## E Microglia-specific mito-Dendra2 expression in UCP2KO



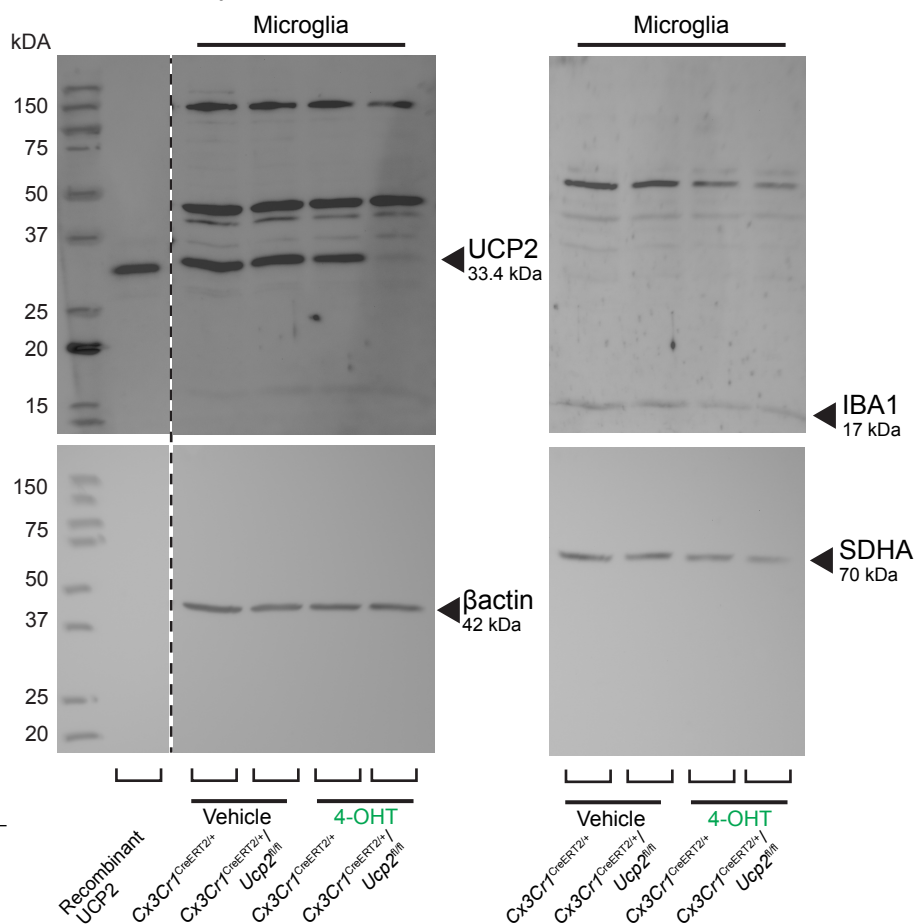
## F Ucp2 transcript level by RT-qPCR



## G Experimental design for primary culture



## H Western blot analysis



## I Quantification of Western blot bands

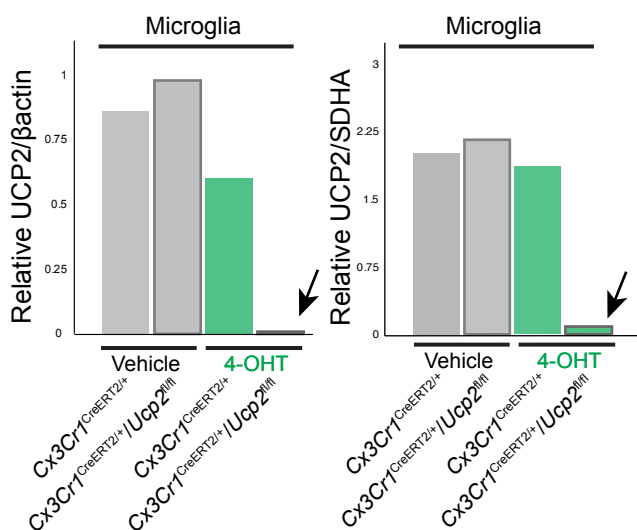


### Figure S4. Selective expression and knockout of UCP2 in retinal microglia, Related to Figure 3

(A-B) Relative fold change expression level of mitochondrial-associated genes (A) and *Ucp2* (B) among retinal cell types. Plotted from available data in Siegert *et. al.* (1). Purple and blue: high and low normalized expression value, respectively. PR: photoreceptors, H: horizontal cells, BP: bipolar cells, Am: amacrine cells, RGC: retinal ganglion cells,  $\mu$ G: microglia.

(C) Timeline for tamoxifen administration to induce mito-Dendra2 expression or in combination UCP2<sup>KO</sup> in microglia used for FACS (fluorescence activated cell sorting).

(D) Boxplot of relative *Ucp2* transcript expression from Dendra2<sup>+</sup>-FACSeD retinal microglia in naïve WT or 5 days ONC WT. Boxplot minimum and maximum: InterQuartile Range (IQR) around median (center line). Whiskers: 1.5 IQRs. Black diamond: outliers outside of 1.5 IQRs. Naïve: grey. ONC: blue. Wilcoxon rank sum test:  $p = 0.0474$ .

(E) Microglial specificity of mito-Dendra2 labeling in UCP2<sup>KO</sup> mouse model. Overview image of immunostained microglia (IBA1, magenta) in the inner plexiform layer (IPL) expressing the mitochondrial label (Dendra2, green) in retinal wholemounts. Scale bar: 50  $\mu$ m.

(F) Relative *Ucp2* transcript expression from tamoxifen-induced naïve WT or naïve UCP2<sup>KO</sup> FACSeD-microglia from the retina. Wilcoxon rank sum test:  $p < 0.0001$ .

(G) Experimental timeline for primary murine mixed glial cultures to obtain microglia and astrocyte-enriched cultures for protein analysis. P0-P3: postnatal day 0 to 3. 4-OHT: 4-hydroxytamoxifen. Next: IBA1-immunostained (magenta) mixed glial culture at day 10 prior to trypsinization. Scale bar: 50  $\mu$ m.

(H) Western blot analysis of UCP2 protein expression (left, top),  $\beta$ -actin loading control (left, bottom), IBA1 microglial marker (right, top), or SDHA (Succinate dehydrogenase complex flavoprotein subunit A) mitochondrial loading control (right, bottom) in primary microglia of either *Cx3cr1*<sup>CreERT2/+</sup> or *Cx3cr1*<sup>CreERT2/+</sup>/*UCP2*<sup>fl/fl</sup> with vehicle or 4-OHT (n = 1). kDa, kilodaltons.

(I) Quantification of UCP2 band intensity relative to  $\beta$ -actin loading control (left) or relative to SDHA (right) mitochondrial loading control.

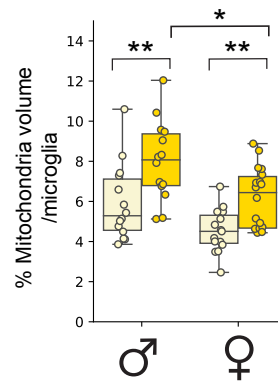
\*  $p < 0.05$ , \*\*\*  $p < 0.001$ . See **Table S9** for retina and cell numbers, statistical tests and corresponding data.

# Figure S5

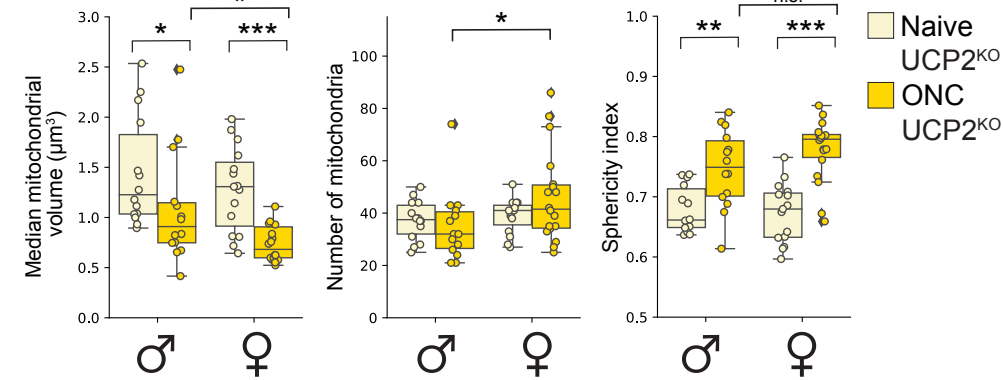
## A Principal component loadings

	PC 1	PC 2
% Mitochondria Perinuclear	0.4915	0.0797
Median mitochondrial volume	-0.3809	0.5161
Number of mitochondria	0.2067	-0.5712
% Mitochondria volume/microglia	0.3184	<b>0.6000</b>
Sholl index	0.5110	0.1991
CD68 volume	0.4563	-0.0379

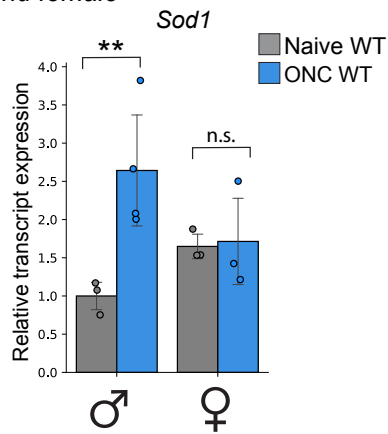
## B Mitochondrial content



## C Mitochondrial connectivity



## D Cellular ROS in WT male and female



## E Mitochondrial ROS in WT ONC male and female

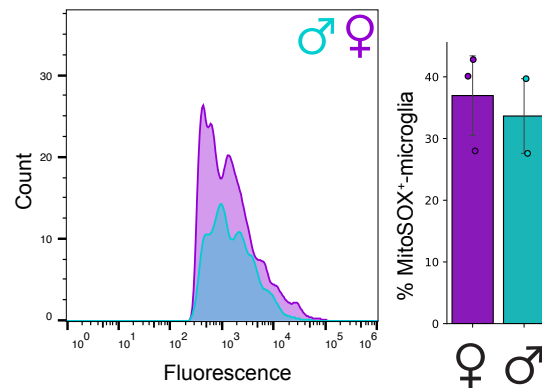


## Figure S5. Sex-separated UCP2<sup>KO</sup> mitochondrial parameters, Related to Figure 5

(A) Table of principal component (PC) loadings from **Figure 5**. Green highlight: Highest loading for PC2.

(B-C) Mitochondrial parameters. Boxplot minimum and maximum: InterQuartile Range (IQR) around median (center line). Whiskers: 1.5 IQRs. Black diamond: outliers outside 1.5 IQRs. Each overlaid point represents data point of a single microglia. Naïve UCP2<sup>KO</sup>: tan. ONC UCP2<sup>KO</sup>: gold.

(B) Percentage of mitochondrial volume per microglial volume. Kruskal-Wallis test:  $p < 0.0001$ . Selected Conover's post-hoc comparisons with Holm p-adjustment: Naïve ♂UCP2<sup>KO</sup> vs. ONC ♂UCP2<sup>KO</sup>,  $p = 0.0076$ ; Naïve ♀UCP2<sup>KO</sup> vs. ONC ♀UCP2<sup>KO</sup>,  $p = 0.0073$ ; ONC ♂UCP2<sup>KO</sup> vs. ONC ♀UCP2<sup>KO</sup>,  $p = 0.0266$ .

(C) Mitochondrial network connectivity determined by median mitochondrial volume (left, Kruskal-Wallis test:  $p < 0.0001$ . Selected Conover's post-hoc comparisons with Holm p-adjustment: Naïve ♂UCP2<sup>KO</sup> vs. ONC ♂UCP2<sup>KO</sup>,  $p = 0.0348$ ; Naïve ♀UCP2<sup>KO</sup> vs. ONC ♀UCP2<sup>KO</sup>,  $p < 0.0001$ ; ONC ♂UCP2<sup>KO</sup> vs. ONC ♀UCP2<sup>KO</sup>,  $p = 0.0303$ ), number of organelles (center, Wilcoxon rank sum test:  $p = 0.0383$ ) and mean sphericity (right, Kruskal-Wallis test:  $p < 0.0001$ . Selected Conover's post-hoc comparisons with Holm p-adjustment: Naïve ♂UCP2<sup>KO</sup> vs. ONC ♂UCP2<sup>KO</sup>,  $p = 0.0029$ ; Naïve ♀UCP2<sup>KO</sup> vs. ONC ♀UCP2<sup>KO</sup>,  $p < 0.0001$ ; ONC ♂UCP2<sup>KO</sup> vs. ONC ♀UCP2<sup>KO</sup>,  $p = 0.2323$ ).

(D) Bar plot depicting relative *Sod1* transcript expression from FACSed mito-Dendra2<sup>+</sup> microglia in naïve WT and ONC WT male and female microglia. Transcript expression relative to male naïve WT. Kruskal-Wallis test:  $p = 0.0269$ . Selected Conover's post-hoc comparisons with Holm p-adjustment: ♂WT Naïve vs. ♂WT ONC:  $p = 0.0026$ , ♀WT Naïve vs. ♀WT ONC:  $p = 0.8554$ .

(E) Frequency plot of MitoSOX fluorescence from FACSed mito-Dendra2<sup>+</sup> retinal microglia for WT ONC male (turquoise) and female (purple). Corresponding bar plot of percentage of microglia that are MitoSOX<sup>+</sup>.

\*\*  $p < 0.01$ , \*\*\*  $p < 0.001$ , <sup>n.s.</sup>  $p > 0.05$ : not significant. See **Table S10** for retina and cell numbers, statistical tests, other post-hoc comparisons and corresponding data.

**Table S11.** Primer sequences, Related to STAR Methods.

<b>Gene</b>	<b>Primer</b>	<b>Sequence</b>	<b>Product length</b>
<b>GAPDH</b>	FW	ACAGCAACTCCCCTCTTC	131 bp
	REV	CATTGTCATACCAGGAAATGAGC	
<b>IBA1</b>	FW	ATGAGGATCTGCCGTCCAAAC	114 bp
	REV	CAAGTTTCTCCAGCATTCGCTTC	
<b>UCP2</b>	FW	AAGTGTTTCGTCTCCAGCC	188 bp
	REV	GGGACCTTCAATCGGCAAGA	
<b>CD68</b>	FW	CCTCTGTTCTTGGGCTATAAG	105 bp
	REV	ATTGAGGAAGGAACTGGTGTAG	
<b>SOD1</b>	FW	CACTTCGAGCAGAAGGCAAGC	186 bp
	REV	ATGCCTCTTTCATCCGCCG	